Version of Record: https://www.sciencedirect.com/science/article/pii/S0368204823000592
Manuscript_de1c0a265e3bb463294a0156d561c737

N, O and F K-edges XAS and DFT combination for the exploration of linkage isomers of coordinated nitric oxide in a ruthenium nitrosyl complex

Artem Mikhailov[a *], Tatyana Asanova[b], Igor Asanov[b], Igor Píš[c], Elena Magnano[c,d], Gennadiy Kostin[b], Dominik Schaniel[a]

*Corresponding author: artem.mikhailov.a@gmail.com

[a] Université de Lorraine, CNRS, CRM2, UMR 7036, Nancy 54000, France

[b] Nikolaev Institute of Inorganic Chemistry, Siberian Branch of the Russian Academy of Sciences, 3 Acad. Lavrentiev Avenue, Novosibirsk 630090, Russian Federation

[c] IOM-CNR, Istituto Officina dei Materiali, AREA Science Park Basovizza, Trieste, 34149, Italy

[d] Department of Physics, University of Johannesburg, PO Box 524, Auckland Park, Johannesburg, 2006, South Africa

Abstract

We report on the experimental investigation of single crystals of *trans*-$[RuNOPy_4F](ClO_4)_2$ (**1**) in its ground state (GS). The X-ray absorption spectroscopy (XAS) spectra measured at the N, O and F K-edges were compared to TDDFT calculations to identify and assign the absorption peaks, and to elucidate the structures of coordinated nitric oxide (NO). Based on a reasonable match of experimental and calculated spectra of GS, the N, O and F K-edges XAS spectra of Ru-ON (MS1) and Ru-η^2-(NO) (MS2) isomers of **1** were calculated. According to the calculations, the energy or/and intensity of the 1s→LUMO, LUMO+1 peaks of N, O or F K-edge changes significantly after GS isomerization to both MS1 and MS2. Current theoretical modeling of the NO linkage isomer in **1** is a background for the future investigation of isomerization process of NO by XAS methods. Since the investigated isomerization occurs in a variety of different nitrosyl complexes, obtained results can be extrapolated to a large family of transition metal nitrosyl compounds.

Introduction

Nitrosyl linkage isomerism is the ability of the nitrosyl ligand NO to be bound to the metal center in different ways – through nitrogen (M-NO), oxygen (M-ON) or by the side bond type (M-η^2-(NO)) [1]. This type of isomerism is characteristic for different metals, but the most prominent results and effects were observed in octahedral ruthenium complexes with general formula L_5Ru-NO. In the ground state (GS) the nitrosyl is coordinated by the nitrogen atom (Ru-NO). The linkage isomers or metastable states (MS1 in case of O-coordinated NO and MS2 in case of side bonding of NO) can be formed after light irradiation of GS. The reaction GS↔MS1/MS2 is reversible and can be driven by light in both directions: blue light excitation induces the direct reaction GS→MS1/MS2, while red light induces the back transfer MS1/MS2→GS. Such linkage photoisomerization can be applied for data storage, for example, since this system can be used as molecular switch [2,3]. The mechanism of photoisomerization is schematically shown in Scheme 1. According to this scheme, light excitation of GS (L_5Ru-NO) leads to MS2 formation (L_5Ru-η^2-(NO) isomer), which then can be excited to the MS1 isomer (L_5Ru-ON). Thus, in the simplest way,

the mechanism of GS isomerization to MS1 is considered as two-step photo-process with MS2 as an intermediate state [4,5]. Experimental data confirmed the two-step mechanism, but experimental information about the nature of transition states (TS) and the transient excited states that are occupied during the isomerization is still missing. A possible mechanism involving the formation of triplet excited states was suggested by density functional theory (DFT) calculations [6–8]. According to work [6], light excitation of GS leads to MS2 formation through a triplet state with following excitation of MS2 to another triplet state and then relaxation to MS1. Nevertheless, experimental evidences are needed to reveal the complicated interplay of excited states during the isomerization process. Knowledge about the intermediate states during photoisomerization is essential to better understand the isomerization mechanism and for identifying the most efficient photoisomerization paths.

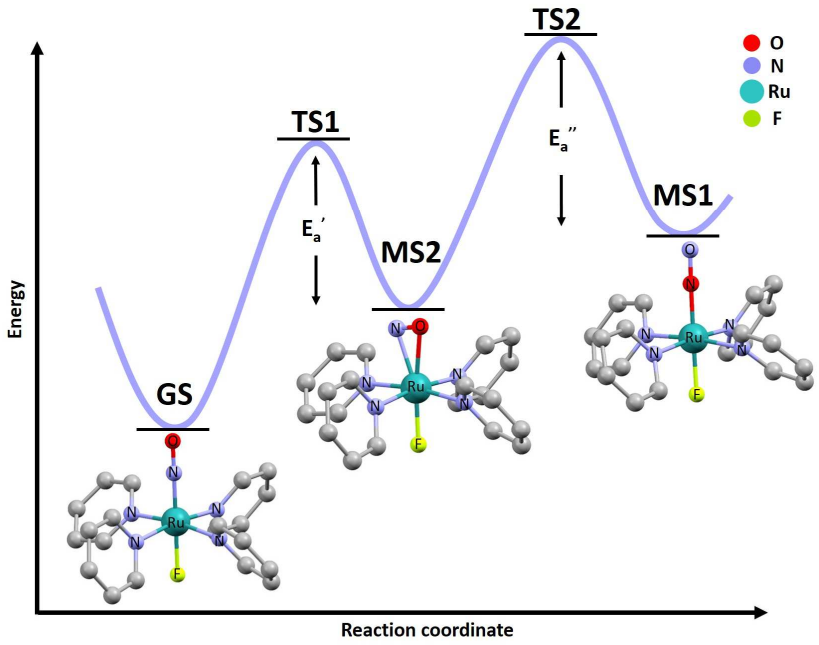

Scheme 1. Schematic photoisomerization mechanism GS→MS2→MS1 on the example of *trans*-$[RuNOPy_4F]^{2+}$. TS1 – a transition state between GS and MS2, TS2 – a transition state between MS2 and MS2.

Time resolved X-ray absorption spectroscopy (TR-XAS) is one of the best techniques to study fast (fs - ms) processes, since this is a direct method to measure changes in the electronic configuration of a chosen atomic core. The main advantage of TR-XAS compared to optical spectroscopic methods is its sensitivity to optically dark transition states [9]. However, before being able to study transient states by time resolved XAS, it is essential to elucidate the signatures of the GS, MS1 and MS2 isomers in order to distinguish these known isomers from potential intermediate states.

Recently, the photoinduced metastable states MS1 and MS2 in *trans*-$[RuNOPy_4F](ClO_4)_2$ (**1**) (Py = pyridine) were characterized by spectroscopic methods and X-ray diffraction (XRD) [4,10,11]. The MS1 isomer was populated by 405-450 nm irradiation of GS, while the MS2 isomer was obtained by 850-1050 nm irradiation of MS1. The bond length Ru-NO was determined to be 1.750(1) Å in GS, while in MS1 the Ru-ON bond length was found to be 1.841(1) Å. In the MS2 isomer the Ru-N-O angle is 80°, and the Ru-N and Ru-O distances are 2.00(2) and 2.09(1) Å, respectively [4]. The Ru-F bond length is also changed after GS→MS1 isomerization from 1.914(1) to 1.898(1) Å. By differential scanning calorimetry it was shown, that MS2 is stable until about 180 K and MS1 decays at around 290 K, while at 80-100 K both states have almost infinite lifetime (GS is fully stable at room temperature). Since GS, MS2 and MS1 isomers in *trans*-

$[RuNOPy_4F](ClO_4)_2$ are well characterized, and achievable populations of MS1 and MS2 are high enough (approximately 90 and 20%, respectively), this complex is a good candidate for the study of the linkage isomers by XAS methods, with particular attention to the changes in the F-Ru-(NO) coordinate of interest, since the biggest structural changes occur in this group.

Thus, in the current work we report XAS spectra of N, O and F K-edges of single crystals of *trans*-$[RuNOPy_4F](ClO_4)_2$ (**1**) in GS. The experimental spectra were explained by means of time-dependent density functional theory (TDDFT) calculations including the description of the TDDFT calculations were then extended to predict the spectra of MS1 and MS2 isomers.

Experimental

Synthesis

The compounds *trans*-$[RuNOPy_4F](ClO_4)_2$ (**1**) and $K_2[RuNOCl_5]$ were synthesized according to the previously published procedures [10,12].

XAS spectroscopy

The XAS spectra at N, O and F K-edges of *trans*-$[RuNOPy_4F](ClO_4)_2$ (**1**) and at N, O K-edges of $K_2[RuNOCl_5]$ were measured at 115 K in total fluorescence yield mode at the BACH beamline of the ELETTRA synchrotron facility (Trieste, Italy) [13,14]. The x-ray fluorescence emission was detected by a micro-channel plate detector (MCP Hamamatsu F4655-13). Single crystals of **1** were attached to the sample holder using a double sided copper adhesive, the single crystal of $K_2[RuNOCl_5]$ was fixed on a Cu foil using a clamp. The measurements chamber pressure was below $1 \cdot 10^{-9}$ mbar during the experiment. The photon energy resolution was set to 70 meV at N K-edge and 150 meV at O and F K-edges. The measured XAS signals from the sample were corrected to the x-ray flux by measuring the photocurrent from a gold mesh inserted into the X-ray beam in front of the sample chamber. The photon energy scale was calibrated using the difference in the kinetic energy of Au 4f core-level measured by photoemission spectroscopy and recorded in the first- and second-order light. The XAS spectra shown in the paper were normalized to the absorption edge jump after a background removal.

Density functional theory calculations

Density functional theory (DFT) calculations were performed in the ADF 2020 package [15]. For the geometry optimization of *trans*-$[RuNOPy_4F]^{2+}$ in GS, MS1 and MS2 (closed-shell electron configurations) in the gas phase, the Perdew-Burke-Ernzerhof (PBE) functional [16] with quadruple-ζ-quality with 4 polarization functions all-electron (QZ4P) basis set [17] was used. The spin-orbit coupling for the Hamiltonian was applied. Initial geometries for the structure optimization were taken from experimental XRD data [4]. Molecular orbitals were calculated for optimized structures on the same level of theory except that a scalar relativistic effect [18] was applied instead of spin-orbit coupling. XAS spectra of K-edges of N, O, F atoms were calculated on the same level of theory with a scalar relativistic effect. XAS spectra were simulated using time-dependent DFT (TDDFT) approach for allowed transitions by the Davidson method [19]. The first 1500 and 500 singlet-singlet electronic excitations were calculated for N, O and F atoms, respectively.

Results and discussion

Experimental XAS spectra of N and O K-edges

The measured N, O XAS spectra of *trans*-[RuNOPy$_4$F](ClO$_4$)$_2$ (**1**) single crystals in GS are shown in Fig. 1. In order to distinguish the peaks related to N and O atoms of the nitrosyl ligand NO without interference of these atoms related to Py ligand (NC_5H_5) and ClO_4^-, the XAS spectra at N and O K-edges of the related complex K_2[RuNOCl$_5$] containing N and O atoms only in the NO ligand were measured.

The N K-edge XAS spectrum of **1** shows three structures at 399.8, 401.6 and 403.8 eV (Fig. 1, *a*). Comparison with the spectrum of K_2[RuNOCl$_5$] indicates that the peak at 401.6 eV is associated with the nitrogen atom of NO ligand (see Fig. 1, *a*). Earlier reports on N K-edge XAS spectra of NO gas adsorbed on different metal surfaces support the assignment [20–22]. The peaks at 399.8 and 403.8 eV are assigned to the nitrogen atoms of the pyridine ligands [23–25], however, the peak at 401.6 eV also might contain a contribution from the pyridines [26]. All these peaks are associated with π-bonds. A broad peak found at higher energy (> 405 eV) is related to σ–bonds. The evolution of the XAS spectra after scanning on the same spot of the sample for a long time (~60 min) is shown in Fig. S1. The X-ray beam induces a decrease of the intensity of mainly the NO peak at 401.6 eV, indicating radiation damage. This modification agrees well with the DFT-calculation: the first LUMO orbitals originate from the Ru-NO group, and their population could potentially lead to a cleavage of the Ru-NO bond [27].

Four main structures at 532.8, 535.6, 537 and 545.5 eV are observed in the O K-edge XAS spectrum of **1** (Fig. 1, *b*). The comparison with the reference spectrum of K_2[RuNOCl$_5$] leads to the conclusion that the peak at 532.8 eV should be assigned to the oxygen atom of NO ligand (Fig. 1, *b*). The other three peaks at 535.6, 537 and 545.5 eV likely are associated with the oxygen atoms of the ClO_4^- anions. This assignment of the peak at 532.8 eV to the oxygen atom of NO is in agreement with literature reports [21,22,28], even though we cannot completely exclude a contribution to this peak originating from the perchlorate anion.

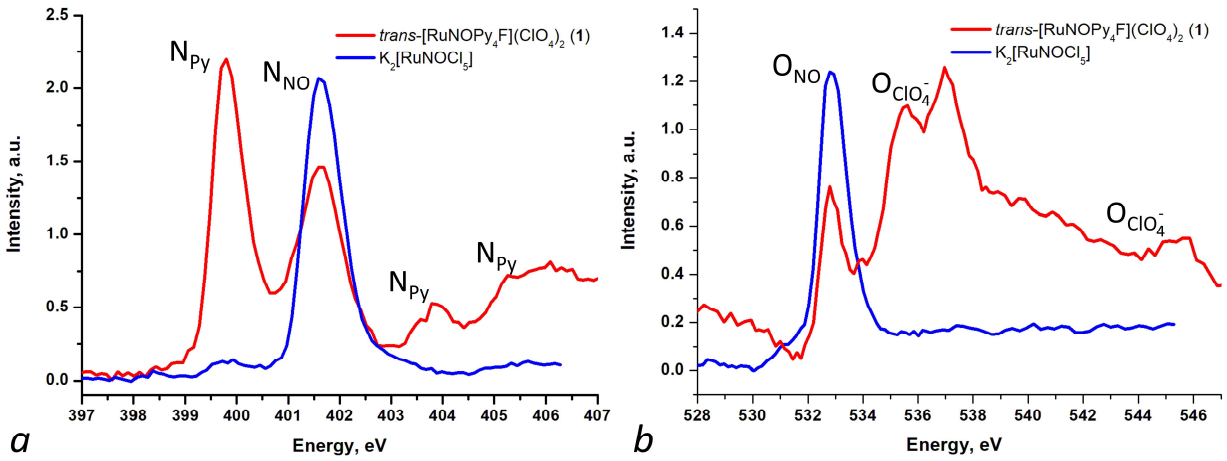

Fig. 1. Comparison of the experimental XAS spectra of N (*a*) and O (*b*) K-edges of K_2[RuNOCl$_5$] and *trans*-[RuNOPy$_4$F](ClO$_4$)$_2$ (**1**).

DFT calculations

To simulate XAS spectra using the TDDFT approach, the GS, MS1 and MS2 structures of **1** (*trans*-[RuNOPy$_4$F]$^{2+}$) were optimized with the PBE functional and QZ4P basis set. The calculated bond lengths and angles agree reasonably well with the experimental data [4], the mean absolute deviations of the

calculated and experimental bond lengths are 0.022, 0.021 and 0.064 Å for GS, MS1 and MS2, respectively (see Table S1). The biggest structural changes occur in the F-Ru-(NO) chain: the Ru-(NO) bond changes from 1.747 Å for GS to 1.838 Å for MS1 and to 1.909/2.157 Å for MS2, which are similar to the experimental data (1.750(1), 1.841(1) and 2.00(2)/2.09(1) Å, respectively).

The most relevant molecular orbitals involved in the electronic transitions appearing in the XAS spectra are shown in Fig. 2 and listed in Tables S2-S5. In case of all isomers the LUMO (118) and LUMO+1 (119) orbitals are composed of Ru d and p orbitals of NO. The average contribution of Ru to these orbitals is approximately 30%, while about 60% originate from the nitrosyl ligand. The remaining contribution to the 118 and 119 antibonding orbitals comes from fluorine p orbitals of the F-Ru-(NO) chain which, however, do not exceed 10%. The majority of the higher lying orbitals shown in Fig. 2 exhibit π*-character related to the pyridine orbitals. The 120, 125 orbitals of GS and 123 orbital of MS1 are composed of Ru d and N, C p-orbitals of pyridine ligands. Overall, the change of the NO linkage in **1** does neither lead to a drastic change of the nature of LUMO and LUMO+1 orbitals nor for the rest higher lying orbitals, which mostly are represented by the π*-pyridine contributions in case of GS, MS1 and MS2.

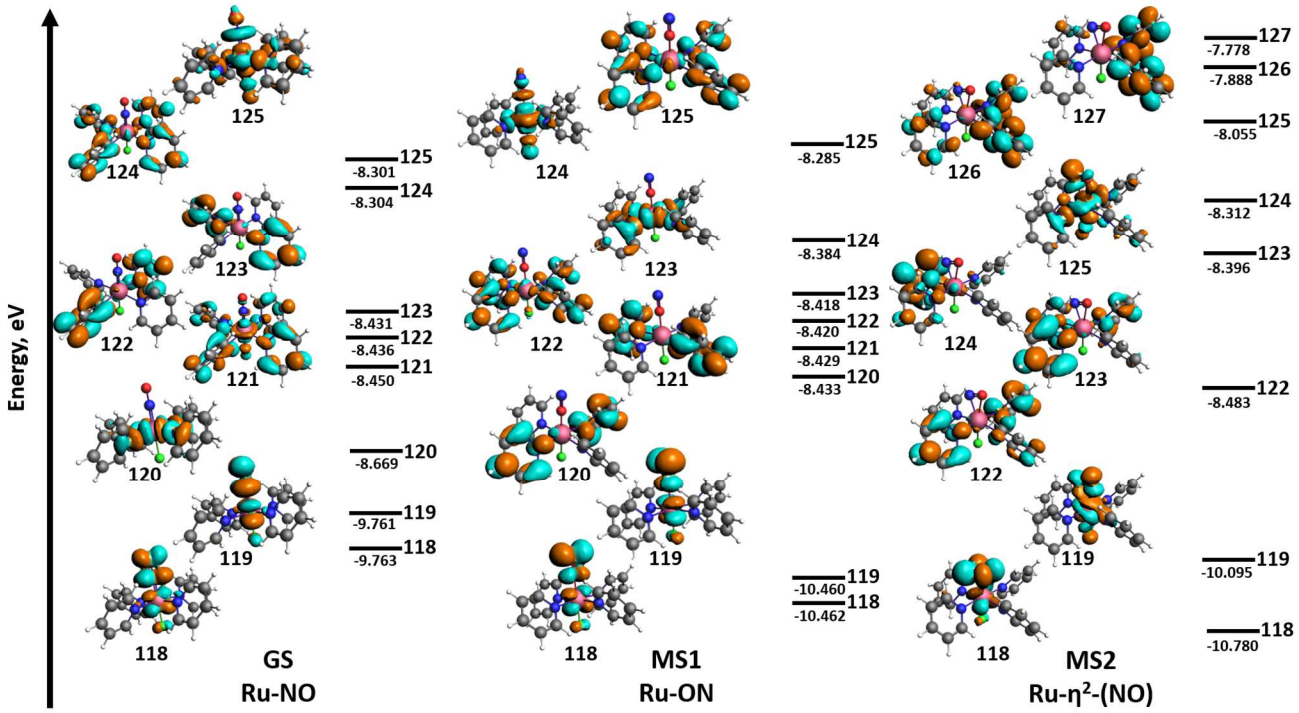

Fig. 2. The main orbitals involved in the transitions of XAS spectra of **1** in GS, MS1 and MS2. The number of LUMO orbital is 118. The energy of the orbitals is shown schematically.

Description of N K-edge XAS spectra

The experimental XAS spectrum at the N K-edge of the single crystals of *trans*-$[RuNOPy_4F](ClO_4)_2$ (**1**) in GS is shown in Fig. 3 together with the TDDFT calculated spectra for GS, MS1 and MS2. The spectrum in the range of 397-407 eV contains four peaks at 399.8, 401.6, 403.8 and 405.7 eV. In order to assign the peaks to certain transitions, the XAS spectrum of *trans*-$[RuNOPy_4F]^{2+}$ in the gas phase was calculated using TDDFT. The calculated spectrum of GS is in good agreement with the experimental data (after having applied an energy shift of +18.9 eV to the calculated spectrum). The electronic transitions contributing to

the XAS peaks and their energies are listed in Table 1. The first structure at 399.8 eV corresponds to the transitions from the 1s orbitals of the nitrogen atoms of the pyridine ligands (N_{Py}) to the 123-125 (LUMO+5-LUMO+7) orbitals (further designated as 1s N_{py}→123-125). These orbitals mainly comprise π-orbitals of pyridine rings with a contribution of ruthenium d-orbitals (see Table S2). The second peak at 401.6 eV is related to the transition from the 1s orbital of nitrogen of the NO ligand (N_{NO}) to the 118, 119 (LUMO, LUMO+1) orbitals (1s N_{NO}→118, 119), which are mainly composed from the antibonding orbitals of the Ru-NO unit (see Table S2). The last two low-intensity peaks at 403.8 and 405.7 eV are assigned to the N_{Py} transitions to the high lying p-orbitals of pyridine ligands (144-146 and 170-173, respectively).

According to the DFT calculations, the change of the Ru-NO (GS) linkage to the Ru-ON (MS1) leads to a drastic change in the XAS spectrum. The calculated spectrum of **1** in MS1 has three structures at 399.8, 403.8 and 406.4 eV (Fig. 3, Table 1). The peak with maximum at 399.8 eV comprises two overlapping transitions: 1s N_{Py}→120-122, 125 and 1s N_{NO}→118, 119. Thus, the NO ligand isomerization leads to a shift of the energy of the 1s N_{NO}→118, 119 transition by -2.1 eV with respect to that in GS. The nature of the 120-122, 125 orbitals is related to the π-systems of pyridines, whereas 118, 119 orbitals arise from the antibonding orbitals of the Ru-ON group. Two remaining peaks at 403.8 and 406.4 eV are also related to the p-orbitals of pyridine rings. Thus, the nature of electronic transitions involved in GS and MS1 is similar, but the energy of the N_{NO} peak is different, being lower in the case of in MS1.

The calculated nitrogen K-edge XAS spectrum of the MS2 isomer shows four structures at 399.8, 402.5, 403.8 and 405.7 eV. Similar to the spectrum of **1** in MS1, the peak with maximum at 399.8 eV contains two transitions 1s N_{Py}→122-125 and 1s N_{NO}→118, 119, as listed in Table 1. The orbitals involved in these transitions are analogous to both GS and MS1 and shown in Table S2. The peak at 402.5 eV reflects the transition 1s N_{NO}→125-127, which was not observed in XAS spectra of GS and MS1. If the transition 1s N_{NO}→118, 119 is mainly due to the electron transfer from 1s orbital of N_{NO} to the antibonding orbitals of Ru-η^2-(NO) group, the 1s N_{NO}→125-127 exhibit an additional transfer to the orbitals of pyridine rings. The last two peaks at 403.8 and 405.7 eV are similar to those in GS and MS1 (see Table 1).

An interesting feature of the calculated spectra is the differing intensity of the peak at 399.8 eV in case of GS, MS1 and MS2. In MS1 and MS2 the intensity is larger compared to the GS, which is due to the shift of the 1s N_{NO}→118, 119 transitions to the lower energy by -2.1 eV inducing an apparent increase in intensity due to the two overlapping peaks (see Fig. 3). The higher intensity of the 1s N_{NO}→118, 119 peak of MS1 compared to that of MS2 is explained by the higher oscillator strength of the transition (0.0806 vs. 0.0554, respectively), which is correlated with the occupancies of the NO orbitals in 118, 119 (72 vs. 54%, respectively, see Table S2). Recently, similar correlation between the intensity of a pre-edge structure in GS, MS1, MS2 and occupancy of the NO orbitals in LUMO(+1) was shown for sodium nitroprusside ($Na_2[FeNO(CN)_5]\cdot 2H_2O$) [29,30]. Thus, from the DFT calculations we may assume a decrease of intensity of the peak at 401.6 eV and corresponding increase of the peak at 399.8 eV after generation of any metastable states due to the shift of the 1s N_{NO}→118, 119 peak.

Table 1. TDDFT calculated transitions in XAS spectra of N, O and F K-edges of **1**.

N K-edge					
GS		MS1		MS2	
E, eV	1s transition	E, eV	1s transition	E, eV	1s transition
399.8	N_{Py}→123-125	399.8	N_{Py}→120-122, 125 N_{NO}→118, 119	399.8	N_{Py}→122-125 N_{NO}→118, 119

401.9	N_{NO}→118, 119	403.8	N_{Py}→142, 144-146	402.5	N_{NO}→125-127
404	N_{Py}→144-146	406.4	N_{Py}→172, 173	403.8	N_{Py}→144-146
405.9	N_{Py}→170-173	-	-	405.7	N_{Py}→170, 171
O K-edge					
532.8	O_{NO}→118, 119	534.5	O_{NO}→118, 119	532.8	O_{NO}→118, 119
F K-edge					
683.2	F→118, 119	682.7	F→118, 119	683.2	F→118, 119
684.8	F→125	685	F→125	685.2	F→125, 126
688	F→134	688.1	F→134	688.4	F→134, 139
690.3, 691.5	F→157, 158	690.5, 691.6	F→157, 158	690.4, 691.7	F→155, 156

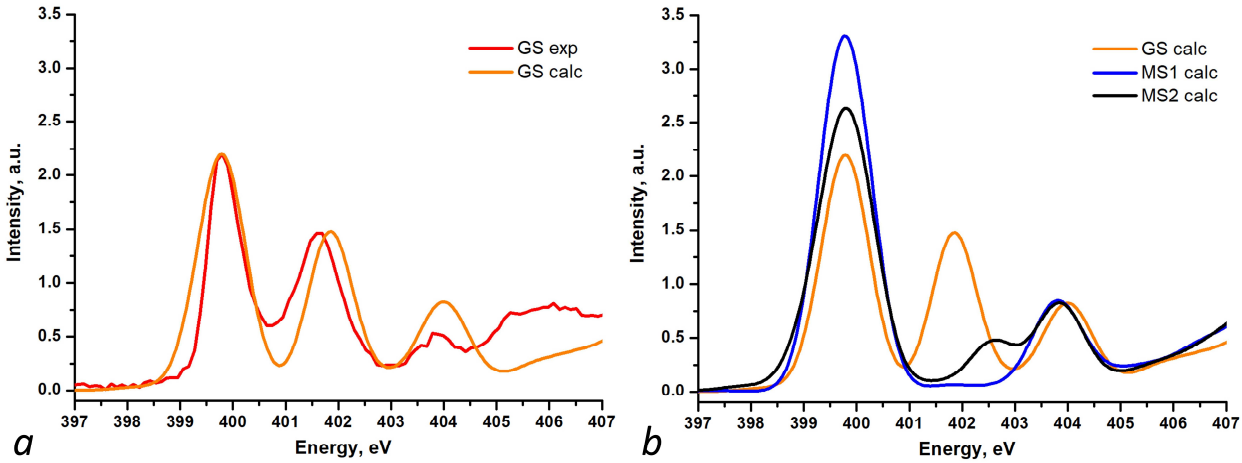

Fig. 3. Experimental (exp) and TDDFT calculated (calc) spectra of N K-edge of **1** in GS, MS1 and MS2. Panel *a* represents comparison of experimental and calculated spectra of **1** in GS, panel *b* shows comparison of calculated GS, MS1 and MS2. Scale factor for energy (X-axis) is +18.9 eV and the Intensity (Y-axis) is multiplied by 0.8 for calculated spectra.

Description of O K-edge XAS spectra

The experimental O K-edge XAS spectrum of the complex in GS shows four structures at 532.8, 535.6, 537 and 545.5 eV (see Fig. 4). It follows from the experimental O K-edge XAS spectrum of $K_2[RuNOCl_5]$ that the peak at 532.8 corresponds to the N-O bond from the ligand NO (O_{NO}), in agreement with literature reports [21,22,28].Therefore the peaks at 535.6, 537 and 545.5 eV in the spectrum of **1** can be assigned to the ClO_4^- anions. Based on the DFT calculations the peak at 532.8 eV of the complex in GS corresponds to the 1s O_{NO}→118, 119 transition. Concerning MS1 and MS2 the nature of the transitions remains the same, the biggest shift of the 1s O_{NO}→118, 119 peak is observed in case of MS1 (see Table 1). Contrary to the N K-edge spectra of linkage isomers, the 1s O_{NO}→118, 119 peak of MS1 is shifted to a higher energy (+1.7 eV), while the peak of MS2 slightly shifts to a lower energy (-0.5 eV). In conclusion, from the theoretical point of view the peak at 532.8 eV should change the amplitude and the position after isomerization of NO.

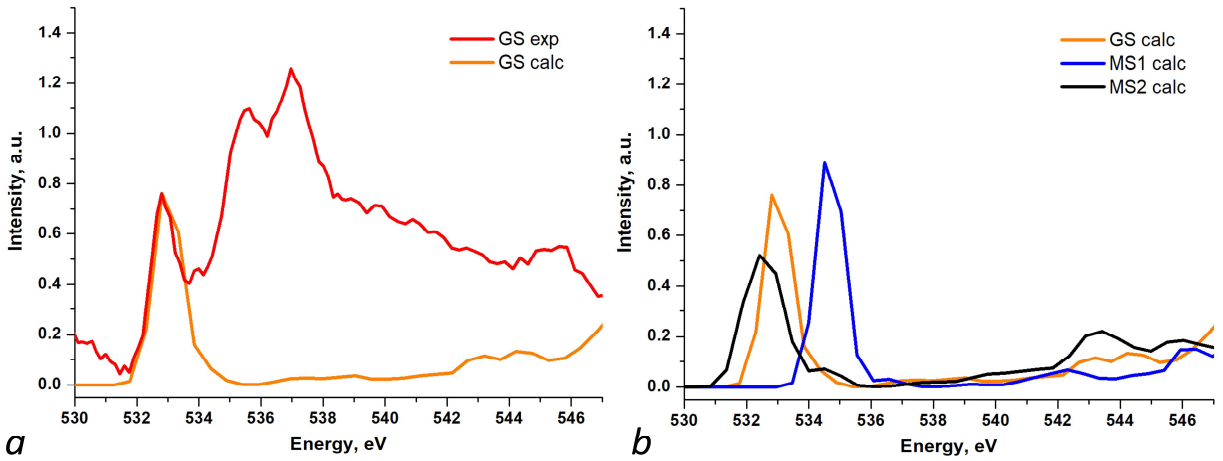

Fig. 4. Experimental (exp) and TDDFT calculated (calc) spectra of O K-edge of **1** in GS, MS1 and MS2. Panel *a* represents comparison of experimental and calculated spectra of **1** in GS, panel *b* shows comparison of calculated GS, MS1 and MS2. Scale factor for energy (X-axis) is +22.3 eV and the intensity (Y-axis) is multiplied by 0.44 for calculated spectra.

Description of F K-edge XAS spectra

Three structures at 684 (shoulder), 684.8 and 692 (broad) eV are observed in the experimental F K-edge XAS spectrum of the complex in GS (see Fig. 5). Regarding the DFT calculations, experimental structures at 684 and 684.8 eV are related to the peaks at 683.2 and 684.8 eV, which are assigned to the 1s F⟶118, 119 and 1s F⟶125 transitions, respectively. The unoccupied orbitals of the Ru-NO unit are mainly involved in these transitions (see Table S2). Three calculated peaks at 688, 690.3 and 691.5 eV are assigned to the broad experimentally observed peak at 692 eV. Calculated peaks are listed in Table 1, and correspond to the 1s transitions to s-orbitals of pyridine ligands (see Table S2). TDDFT simulated spectra of MS1 and MS2 show similar patterns and the corresponding transitions are listed in Table 1. Since nitrosyl isomerization affects the Ru-F bond length less than the Ru-(NO) bond length [4,11,31], the calculated spectra do not show such drastic changes as observed in the N and O K-edges. The biggest shift to lower energy is observed for the 1s F⟶118, 119 peak of MS1 (-0.5 eV), whilst the peak at 684.8 eV noticeably changes the amplitude in different states (Fig. 5).

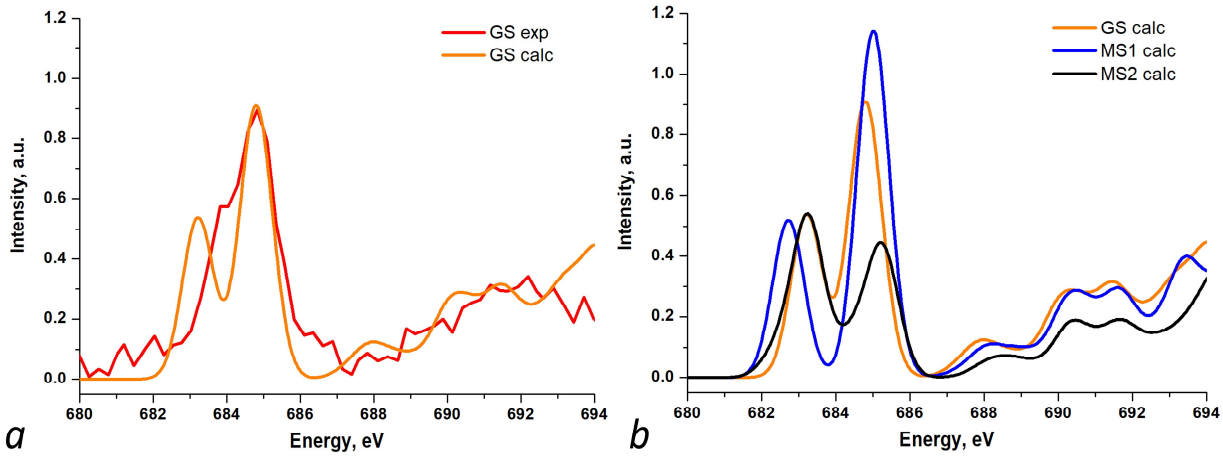

Fig. 5. Experimental (exp) and TDDFT calculated (calc) spectra of F K-edge of **1** in GS, MS1 and MS2. Panel *a* represents comparison of experimental and calculated spectra of **1** in GS, panel *b* shows comparison of calculated GS, MS1 and MS2. Scale factor for X is +26.8 eV and for Y is multiplied by 100 for calculated spectra.

From the TDDFT data the energy shift of the 1s $N_{NO}/O_{NO}/F \rightarrow$118, 119 (LUMO, LUMO+1) peaks is expected after GS isomerization to MS1 and MS2 (see Figs. 3-5). In case of the N K-edge XAS spectra the NO isomerization from GS to MS1 and MS2 leads to downshift of about -2.1 eV of the 1s $N_{NO} \rightarrow$118, 119 peak. In case of the O K-edge XAS spectra, the GS isomerization to MS1 leads to an upshift of about 1.7 eV, whereas the generation of MS2 leads to a downshift of about -0.5 eV. Note that the nature of these transitions (1s $N_{NO}/O_{NO} \rightarrow$118, 119) is very similar, thus the energetic positions of the 118 and 119 orbitals should indicate at least the expected direction of the shift. However, the consideration of those energies alone would not explain the shift, since from that only a downshift would be expected (see Fig. 2, the energies of 118/119 for GS, MS1, MS2 are -9.763/-9.761, -10.462/-10.460, -10.780/-10.095 eV, respectively). Hence, the energies of the 1s orbitals must be considered as well in order to explain the resulting shift of the peaks. In Table 2 the energies of the 1s orbitals related to NO, F ligands along with the energies of 118 (LUMO), 119 LUMO+1 orbitals and 1s→118, 119 transitions are presented. From Table 2, it is clear that the energy of the 1s orbital varies for different isomers and compensates the energy change of 118, 119 orbitals. For example, in case of the N K-edge the energy gap between 1s and 118, 119 orbitals is higher for GS than in MS1/MS2 by 1.6/1.7 eV, which is in accordance with the energy difference of the corresponding 1s→118, 119 transitions (2.1/2.1 eV). In case of the O K-edge the 1s→118, 119 energy gap is different, leading to the difference between GS and MS1/MS2 gaps of -1.6/0.8 eV.

A possible origin of the decrease of the energy of antibonding orbitals 118 (LUMO) in the sequence GS (-9.763 eV), MS1 (-10.462 eV) and MS2 (-10.780 eV) is the elongation of the Ru-(NO) bond length, which are 1.747, 1.838 and 1.909/2.157 Å, respectively. Thus, weakening of the Ru-(NO) bond should facilitate the occupation of antibonding LUMO orbitals. The change of the energy of 1s orbitals might be attributed to a redistribution of the Hirshfeld charges on atoms after NO isomerization (see Table S6). The biggest difference in the energy of 1s orbitals of N_{NO}/O_{NO} and their charges is observed between GS and MS1 isomers. The overall charge on NO changes from 0.099 (GS) to 0.16 (MS1) with corresponding decrease of the charge on Ru atom from 0.493 (GS) to 0.468 (MS1), indicating the transfer of electron density from NO ligand to Ru. In case of the MS2 isomer the decrease of the charge on both Ru (0.486) and NO (0.073) occurs, which lead to the increase of the charges on fluoride and pyridine ligands (Table S6).

Table 2. The comparison of 1s, 118 (LUMO), 119 (LUMO+1) energies and the energies of 1s→118, 119 transitions of GS, MS1 and MS2.

Energies of 1s orbitals, eV			
	GS	MS1	MS2
1s N_{NO}	-391.966	-391.026	-391.324
1s O_{NO}	-520.591	-522.916	-520.810
1s F	-665.535	-665.721	-665.781
Difference energy of 1s and 118/119 orbitals (ΔE), eV			
$\lvert$1s N_{NO} – 118/119$\rvert$	382.203	380.564	380.544
$\lvert$1s O_{NO} – 118/119$\rvert$	510.828	512.454	510.03

|1s F – 118/119|	655.772	655.259	655.686
	Difference of ΔE energies, eV	Difference of 1s→118, 119 peaks from TDDFT, eV	
	$\Delta E_{GS}-\Delta E_{MS1}/\Delta E_{GS}-\Delta E_{MS2}$	$(1s\rightarrow 118, 119)_{GS}-(1s\rightarrow 118, 119)_{MS1}$ / $(1s\rightarrow 118, 119)_{GS}-(1s\rightarrow 118, 119)_{MS2}$	
N K-edge	1.6/1.7	2.1/2.1	
O K-edge	-1.6/0.8	-1.7/0.5	
F K-edge	0.5/0.1	0.5/0	

Conclusions

The experimental N, O and F K-edge XAS spectra of single crystals of *trans*-$[RuNOPy_4F](ClO_4)_2$ (**1**) in GS were measured. In order to distinguish XAS structures related to the coordinated NO molecule, the N and O K-edge XAS spectra were compared with those of related complex $K_2[RuNOCl_5]$. Subsequently, TDDFT calculated N, O and F K-edge XAS spectra allowed for the assignment of the observed transition exhibiting a relatively good quantitative agreement with experimental data. According to the analysis of molecular orbitals, the 118 (LUMO) and 119 (LUMO+1) are related to the unoccupied orbitals of the Ru-NO group. The next higher lying orbitals are mainly represented by the π-systems of pyridine ligands. In N, O K-edge XAS spectra of **1** the structures which correspond to the 1s N_{NO}/O_{NO} →118, 119 transitions are found at 401.6/ 532.8 eV, respectively. In F K-edge XAS spectra the peak of 1s F→118, 119 transition is observed at 684 eV. It is important to emphasize that these peaks are the most interesting in terms of investigation of NO isomerization, since the biggest structural changes occur in the F-Ru-(NO) chain after formation of any linkage isomer. Given a decent match of experimental and calculated XAS spectra of **1** in GS, the N, O and F K-edge XAS spectra of MS1 and MS2 isomers were simulated using TDDFT. In the calculated N K-edge XAS spectra of MS1 and MS2 the shift of the 1s N_{NO}→118, 119 peaks with respect to that of GS by -2.1 eV is observed. The calculated O K-edge spectra exhibit a different behavior: the spectrum of MS1 is characterized by the shift of the 1s O_{NO}→118, 119 peak to higher energy by +1.7 eV, whereas a downshift by -0.5 eV is observed for MS2. The 1s F→118, 119 transition of the MS1 F K-edge XAS spectrum exhibits a downshift by -0.5 eV, whereas that peak of MS2 has the same energy with respect to GS. The observed differences of the calculated shift of these peaks were interpreted by a significant change of the energies of the 1s levels of N, O, F atoms of NO and F ligands in different linkage isomers. Thus, based on the experimental XAS spectra of GS of **1**, the spectra of MS1 and MS2 linkage isomers were calculated using TDDFT approach. Subsequently, these results will allow to prepare the more complex study of the mechanism of nitrosyl photoisomerization by time resolved XAS.

Acknowledgement

XAS measurements were carried out on an approved proposal (20210330) of BACH beamline of ELETTRA synchrotron, Italy. The work has been supported by grant of ANR (grant no. ANR-21-CE30-0045-01) and Russian Science Foundation (22-43-09001, https://rscf.ru/project/22-43-09001/) in the part of XAS and DFT calculations, respectively. The research was supported by the Ministry of Science and Higher Education of the Russian Federation, N 121031700315-2 in the part of synthesis and characterization of ruthenium complexes. A. M. is grateful for financial support from the Metchnikov bourse program 2021. E.M. and I.P. acknowledge support from the EUROFEL project (RoadMap Esfri) and Federico Salvador of IOM-CNR for technical support.

References

[1] P. Coppens, I. Novozhilova, A. Kovalevsky, Photoinduced Linkage Isomers of Transition-Metal Nitrosyl Compounds and Related Complexes, Chem. Rev. 102 (2002) 861–884. https://doi.org/10.1021/cr000031c.

[2] D. Schaniel, M. Imlau, T. Weisemoeller, T. Woike, K.W. Krämer, H.-U. Güdel, Photoinduced Nitrosyl Linkage Isomers Uncover a Variety of Unconventional Photorefractive Media, Adv. Mater. 19 (2007) 723–726. https://doi.org/10.1002/adma.200601378.

[3] I. Stepanenko, M. Zalibera, D. Schaniel, J. Telser, V.B. Arion, Ruthenium-nitrosyl complexes as NO-releasing molecules, potential anticancer drugs, and photoswitches based on linkage isomerism, Dalt. Trans. 51 (2022) 5367–5393. https://doi.org/10.1039/D2DT00290F.

[4] A.A. Mikhailov, E. Wenger, G.A. Kostin, D. Schaniel, Room-Temperature Photogeneration of Nitrosyl Linkage Isomers in Ruthenium Nitrosyl Complexes, Chem. – A Eur. J. 25 (2019) 7569–7574. https://doi.org/10.1002/chem.201901205.

[5] L. Khadeeva, W. Kaszub, M. Lorenc, I. Malfant, M. Buron-Le Cointe, Two-Step Photon Absorption Driving the Chemical Reaction in the Model Ruthenium Nitrosyl System [Ru(py) 4 Cl(NO)](PF 6) 2 · 1 / 2 H 2 O, Inorg. Chem. 55 (2016) 4117–4123. https://doi.org/10.1021/acs.inorgchem.5b02572.

[6] J. Sanz García, F. Alary, M. Boggio-Pasqua, I.M. Dixon, I. Malfant, J.-L. Heully, Establishing the Two-Photon Linkage Isomerization Mechanism in the Nitrosyl Complex trans -[RuCl(NO)(py) 4] 2+ by DFT and TDDFT, Inorg. Chem. 54 (2015) 8310–8318. https://doi.org/10.1021/acs.inorgchem.5b00998.

[7] F. Talotta, J.-L. Heully, F. Alary, I.M. Dixon, L. González, M. Boggio-Pasqua, Linkage Photoisomerization Mechanism in a Photochromic Ruthenium Nitrosyl Complex: New Insights from an MS-CASPT2 Study, J. Chem. Theory Comput. 13 (2017) 6120–6130. https://doi.org/10.1021/acs.jctc.7b00982.

[8] F. Talotta, M. Boggio-Pasqua, L. González, Early Relaxation Dynamics in the Photoswitchable Complex trans -[RuCl(NO)(py) 4] 2+, Chem. – A Eur. J. 26 (2020) 11522–11528. https://doi.org/10.1002/chem.202000507.

[9] A.A. Cordones, J.H. Lee, K. Hong, H. Cho, K. Garg, M. Boggio-Pasqua, J.J. Rack, N. Huse, R.W. Schoenlein, T.K. Kim, Transient metal-centered states mediate isomerization of a photochromic ruthenium-sulfoxide complex, Nat. Commun. 9 (2018). https://doi.org/10.1038/s41467-018-04351-0.

[10] G.A. Kostin, A.A. Mikhailov, N. V Kuratieva, D.P. Pishchur, A.N. Makhinya, High thermal stability of the Ru–ON (MS1) linkage isomer of the ruthenium nitrosyl complex [RuNO(Py) 4 F](ClO 4) 2 with the trans NO–Ru–F coordinate, New J. Chem. 42 (2018) 18928–18934. https://doi.org/10.1039/C8NJ04620D.

[11] A.A. Mikhailov, T. Woike, A. Gansmüller, D. Schaniel, G.A. Kostin, Photoinduced linkage isomers in a model ruthenium nitrosyl complex: Identification and assignment of vibrational modes, Spectrochim. Acta Part A Mol. Biomol. Spectrosc. 263 (2021) 120217. https://doi.org/10.1016/j.saa.2021.120217.

[12] V.A. Emel'yanov, M.A. Fedotov, A. V. Belyaev, S. V. Tkachev, A multinuclear magnetic

resonance study of transformations of ruthenium(II) nitrosyl chloride complexes in aqueous solutions, Russ. J. Inorg. Chem. 58 (2013) 956–963. https://doi.org/10.1134/s003602361308007x.

[13] M. Zangrando, M. Finazzi, G. Paolucci, G. Comelli, B. Diviacco, R.P. Walker, D. Cocco, F. Parmigiani, BACH, the beamline for advanced dichroic and scattering experiments at ELETTRA, Rev. Sci. Instrum. 72 (2001) 1313. https://doi.org/10.1063/1.1334626.

[14] M. Zangrando, M. Zacchigna, M. Finazzi, D. Cocco, R. Rochow, F. Parmigiani, Polarized high-brilliance and high-resolution soft x-ray source at ELETTRA: The performance of beamline BACH, Rev. Sci. Instrum. 75 (2004) 31–36. https://doi.org/10.1063/1.1634355.

[15] G. te Velde, F.M. Bickelhaupt, E.J. Baerends, C. Fonseca Guerra, S.J.A. van Gisbergen, J.G. Snijders, T. Ziegler, Chemistry with ADF, J. Comput. Chem. 22 (2001) 931–967. https://doi.org/10.1002/jcc.1056.

[16] M. Ernzerhof, G.E. Scuseria, Assessment of the Perdew–Burke–Ernzerhof exchange-correlation functional, J. Chem. Phys. 110 (1999) 5029–5036. https://doi.org/10.1063/1.478401.

[17] E. Van Lenthe, E.J. Baerends, Optimized Slater-type basis sets for the elements 1-118, J. Comput. Chem. 24 (2003) 1142–1156. https://doi.org/10.1002/jcc.10255.

[18] J. Li, G. Schreckenbach, T. Ziegler, A Reassessment of the First Metal-Carbonyl Dissociation Energy in M(CO)4 (M = Ni, Pd, Pt), M(CO)5 (M = Fe, Ru, Os), and M(CO)6 (M = Cr, Mo, W) by a Quasirelativistic Density Functional Method, J. Am. Chem. Soc. 117 (1995) 486–494. https://doi.org/10.1021/ja00106a056.

[19] A. Rosa, E.J. Baerends, S.J.A. van Gisbergen, E. van Lenthe, J.A. Groeneveld, J.G. Snijders, Electronic Spectra of M(CO) 6 (M = Cr, Mo, W) Revisited by a Relativistic TDDFT Approach, J. Am. Chem. Soc. 121 (1999) 10356–10365. https://doi.org/10.1021/ja990747t.

[20] T. Saito, M. Imamura, N. Matsubayashi, K. Furuya, T. Kikuchi, H. Shimada, Geometric and electronic structures of NO adsorbed on Ni, Rh and Pt studied by using near edge X-ray absorption fine structure (NEXAFS) and resonant photoemission spectroscopy, J. Electron Spectros. Relat. Phenomena. 119 (2001) 95–105. https://doi.org/10.1016/S0368-2048(01)00278-X.

[21] T. Saito, F. Esaka, K. Furuya, T. Kikuchi, M. Imamura, N. Matsubayashi, H. Shimada, XAS and XPS studies on molecular and dissociative adsorption of nitric oxide on Rh, J. Electron Spectros. Relat. Phenomena. 88–91 (1998) 763–766. https://doi.org/10.1016/S0368-2048(97)00167-9.

[22] F. Esch, T. Greber, S. Kennou, A. Siokou, S. Ladas, R. Imbihl, The formation of a NO-NH3 coadsorption complex on a Pt(l11) surface: a NEXAFS study, Catal. Letters. 38 (1996) 165–170. https://doi.org/10.1007/BF00806563.

[23] J.T. Lukens, I.M. DiMucci, T. Kurogi, D.J. Mindiola, K.M. Lancaster, Scrutinizing metal–ligand covalency and redox non-innocence via nitrogen K-edge X-ray absorption spectroscopy, Chem. Sci. 10 (2019) 5044–5055. https://doi.org/10.1039/C8SC03350A.

[24] M. Nagasaka, H. Yuzawa, N. Kosugi, Intermolecular Interactions of Pyridine in Liquid Phase and Aqueous Solution Studied by Soft X-ray Absorption Spectroscopy, Zeitschrift Für Phys. Chemie. 232 (2018) 705–722. https://doi.org/10.1515/zpch-2017-1054.

[25] A. Baiardi, M. Mendolicchio, V. Barone, G. Fronzoni, G.A. Cardenas Jimenez, M. Stener, C. Grazioli, M. de Simone, M. Coreno, Vibrationally resolved NEXAFS at C and N K-edges of pyridine, 2-fluoropyridine and 2,6-difluoropyridine: A combined experimental and theoretical assessment, J. Chem. Phys. 143 (2015) 204102. https://doi.org/10.1063/1.4935715.

[26] A. Vairavamurthy, S. Wang, Organic Nitrogen in Geomacromolecules: Insights on Speciation and Transformation with K-edge XANES Spectroscopy, Environ. Sci. Technol. 36 (2002) 3050–3056. https://doi.org/10.1021/es0155478.

[27] M.J. Rose, P.K. Mascharak, Photoactive ruthenium nitrosyls: Effects of light and potential application as NO donors, Coord. Chem. Rev. 252 (2008) 2093–2114. https://doi.org/10.1016/j.ccr.2007.11.011.

[28] F. Frati, M.O.J.Y. Hunault, F.M.F. de Groot, Oxygen K-edge X-ray Absorption Spectra, Chem. Rev. 120 (2020) 4056–4110. https://doi.org/10.1021/acs.chemrev.9b00439.

[29] D.T. Kamgne, B.T. Sendja, D.O. de Souza, T. Woike, G. Aquilanti, D. Schaniel, X-ray Absorption Spectroscopy for the Characterization of Photoinduced Linkage Isomers in Single Crystals: Experimental Setup and XANES Results**, ChemPhotoChem. (2022). https://doi.org/10.1002/cptc.202200221.

[30] D. Tchana Kamgne, B. Thiodjio Sendja, D. Oliveira de Souza, D. Schaniel, G. Aquilanti, An experimental XAS and ab initio approach to describe the electronic and local structure of sodium nitroprussiate single crystals, J. Mol. Struct. 1245 (2021) 131119. https://doi.org/10.1016/j.molstruc.2021.131119.

[31] A. Gansmüller, A.A. Mikhailov, G.A. Kostin, J. Raya, C. Palin, T. Woike, D. Schaniel, Solid-State Photo-NMR Study on Light-Induced Nitrosyl Linkage Isomers Uncovers Their Structural, Electronic, and Diamagnetic Nature, Anal. Chem. 94 (2022) 4474–4483. https://doi.org/10.1021/acs.analchem.1c05564.

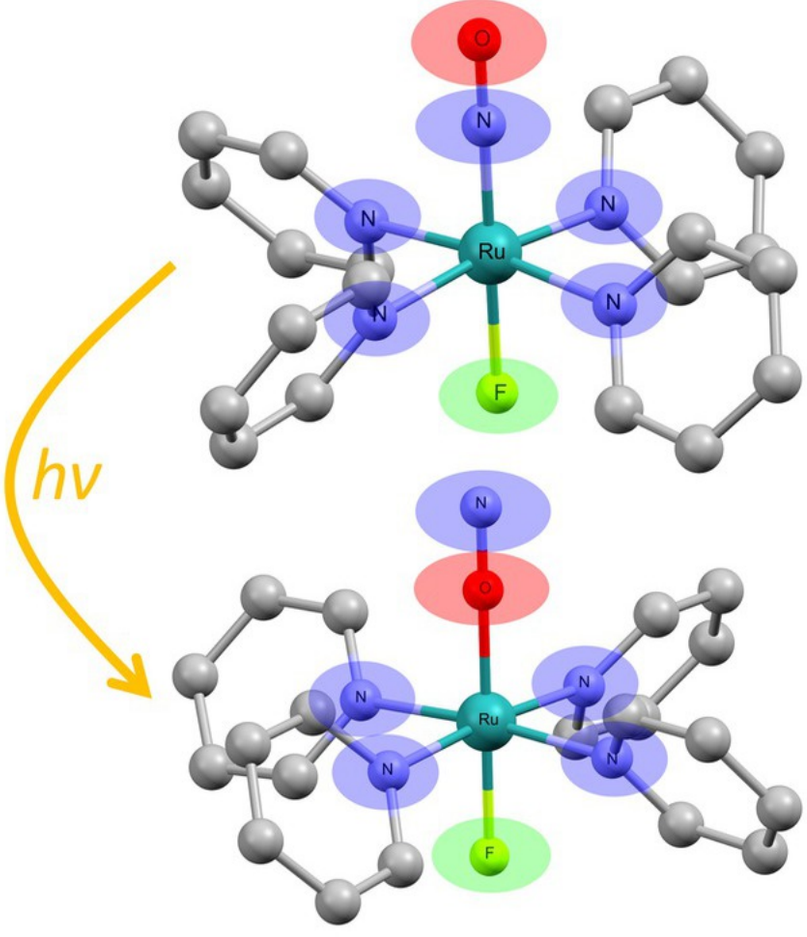
hv
O
N
N
N
Ru
N
N
F
N
O
N
N
Ru
N
N
F

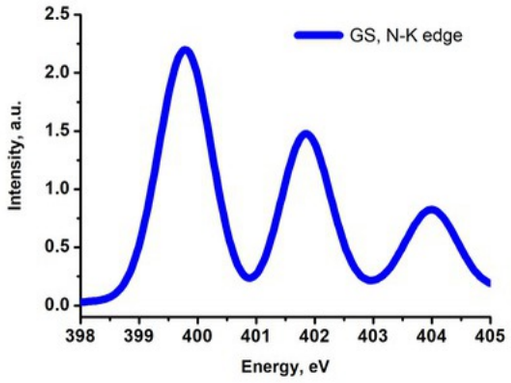
GS, N-K edge
Intensity, a.u.
Energy, eV

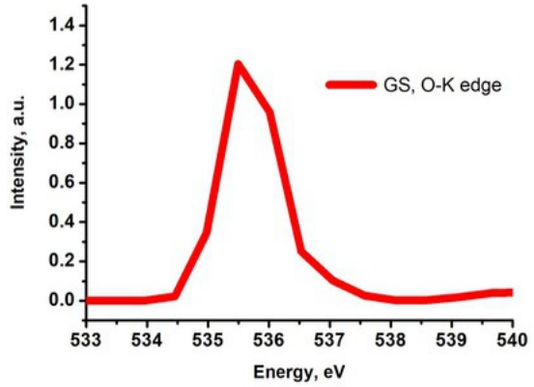
GS, O-K edge
Intensity, a.u.
Energy, eV

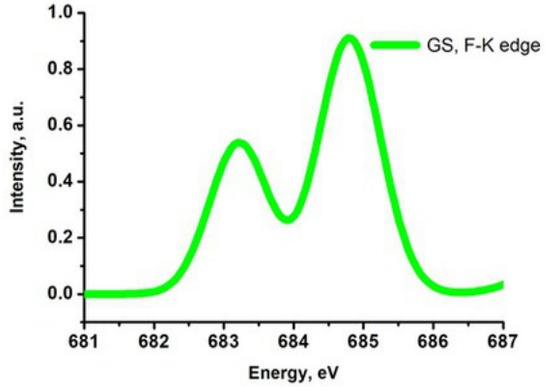
GS, F-K edge
Intensity, a.u.
Energy, eV

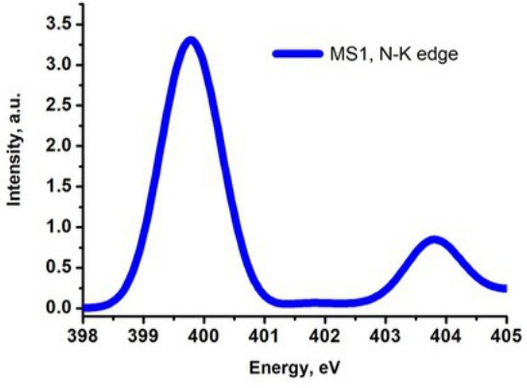
MS1, N-K edge
Intensity, a.u.
Energy, eV

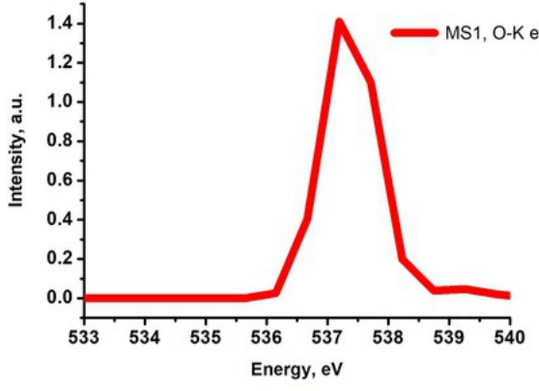
MS1, O-K edge
Intensity, a.u.
Energy, eV

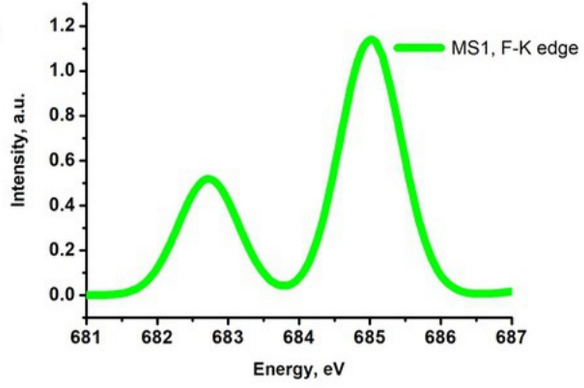
MS1, F-K edge
Intensity, a.u.
Energy, eV